



EUROfusion

WPPMI-CPR(17) 17960

O Costa et al.

Effect of DEMO Load Cases on Rectangular Bellows Design

Preprint of Paper to be submitted for publication in Proceeding of
26th International Conference Nuclear Energy for New Europe -
NENE2017



This work has been carried out within the framework of the EUROfusion Consortium and has received funding from the Euratom research and training programme 2014-2018 under grant agreement No 633053. The views and opinions expressed herein do not necessarily reflect those of the European Commission.

This document is intended for publication in the open literature. It is made available on the clear understanding that it may not be further circulated and extracts or references may not be published prior to publication of the original when applicable, or without the consent of the Publications Officer, EUROfusion Programme Management Unit, Culham Science Centre, Abingdon, Oxon, OX14 3DB, UK or e-mail Publications.Officer@euro-fusion.org

Enquiries about Copyright and reproduction should be addressed to the Publications Officer, EUROfusion Programme Management Unit, Culham Science Centre, Abingdon, Oxon, OX14 3DB, UK or e-mail Publications.Officer@euro-fusion.org

The contents of this preprint and all other EUROfusion Preprints, Reports and Conference Papers are available to view online free at <http://www.euro-fusionscipub.org>. This site has full search facilities and e-mail alert options. In the JET specific papers the diagrams contained within the PDFs on this site are hyperlinked

Effect of DEMO Load Cases on Rectangular Bellows Design

Oriol Costa Garrido, Boštjan Končar

Jožef Stefan Institute, Reactor Engineering Division
Jamova cesta 39
SI-1000 Ljubljana, Slovenia
oriol.costa@ijs.si, bostjan.koncar@ijs.si

Richard Brown, Christian Bachmann

PPPT, PMU, Eurofusion
Boltzmannstrasse 2
85748 Garching, Germany
richard.brown@euro-fusion.org, christian.bachmann@euro-fusion.org

ABSTRACT

A preliminary dimensioning of the DEMO upper port cryostat bellows is performed with the available standardized analytical procedures for rectangular bellows. The aim of the analyses is to find out if there exist sets of bellows parameters that fulfil the design constraints and the available space dimensions for the bellows in the DEMO plant model. The development of an in-house tool for the optimization of bellows parameters has been initiated and a sensitivity analysis of load cases, materials and dimensions of the bellows is performed. The results of the analyses show that, with the current design assumptions, the available sets of bellows parameters are very dependent on the inputs given the challenging dimensions and loadings of the DEMO bellows. Additionally, it has been found that the high mass of some of the available bellows may actually represent an important design constraint.

1 INTRODUCTION

It is foreseen that the connection between the vacuum vessel (VV) ports and the cryostat in the DEMO fusion reactor will be performed with bellows expansion joints, named as cryostat bellows. The cryostat bellows should accommodate the relative displacements between the two connected components that occur due to thermal expansions or seismic motion. Additionally, cryostat bellows should also maintain the cryostat vacuum from the pressure inside the VV port.

The American Society of Mechanical Engineers code (ASME) [1] and the standards for the Expansion Joint Manufacturers Association (EJMA) [2] provide rules for design of standard bellows. The design of more complex bellows under challenging loadings, such as those for ITER [3] and Wendelstein 7-X [4] fusion reactors, typically require additional industrial expertise due to the limitations of the available rules.

The initial activities on bellows design for DEMO, currently at the pre-conceptual stage, include the screening of the available rules [5]. To this end, the aim of the paper is to present the initial dimensioning of the DEMO upper port cryostat bellows using the available standardized analytical procedures for rectangular bellows. The work has been performed in 2016 at Jožef Stefan Institute within the “initial definition of cryostat bellows” task of the “Project Management and Integration” (PMI) work package of EUROfusion [6].

In Section 2, the analytical procedure for design of rectangular bellows is described. Section 3 presents the DEMO upper port dimensions, load case scenarios and the preliminary results of the bellows' design. In Section 4, the conclusions of the work performed are drawn.

2 ANALYTICAL PROCEDURE FOR RECTANGULAR BELLOWS DESIGN

This section describes the analytical procedure for single ply and unreinforced rectangular universal bellows, mainly following the EJMA standard [2], employed for the initial dimensioning of the DEMO cryostat bellows. Taken as the initial assumption, this is the best available procedure for the assumed shape of the bellows (see Fig. 3 in Section 3). The procedure for the bellows working temperature below the creep limit is also assumed.

2.1 Bellows parameters

The parameters of a "U" shape convolution are depicted in Fig. 1-left. These include the thickness (t), pitch (q), height (w) and mean radius (r_m). The bellows are thus described by the shape of their convolutions, the number of convolutions in one bellows (N) and the connector length (L_c), Fig. 1-right, which defines the total length of the bellows expansion joint, L_u . The length of additional material to connect with the components is named as tangent, L_t . The cross sectional dimensions in rectangular bellows are defined by the inner dimensions of the long (L_l) and short (L_s) sides, as shown in Fig. 1-right.

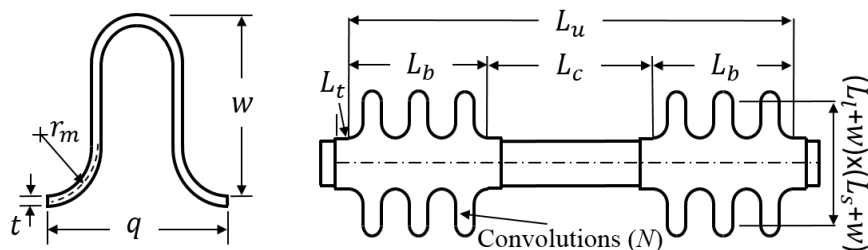


Figure 1: Convolution parameters (left) and length dimensions (right)

2.2 Bellows' stresses, displacements and design constraints

The list of convolution's stresses covered by EJMA standard is given in Table 1. The naming convention of stress components follows the directions relative to the convolution depicted in Fig. 2. Note that in Table 1, the length of the side needed to calculate the membrane and bending stresses in the longitudinal direction varies depending on the side where the stress is calculated. It is worth mentioning that the stress components due to pressure loads in Table 1 are dependent on the input pressure (P) and geometry but they are material independent. The geometry dependent variables such as the convolution cross sectional area (A_c) and the moment of inertia (I) can be found in the nomenclature of the EJMA standard [2]. The only stress considered by EJMA due to displacement load (Table 1) is linearly dependent on the Young Modulus, E_b , and the total equivalent axial displacement of the convolution, e . The latter is defined in Table 2.

The K_u factor in the expression of the equivalent axial movement is defined in Fig. 4-1 of the EJMA standard [2]. The maxima, compression and extension, displacements per convolution are defined by simple geometrical restrictions and are also given in Table 2. The input displacement loads U_i for the bellows are defined in Section 3.

According to the analytical procedure, the stresses and displacements defined in Tables 1 and 2 have to fulfil the design constraints presented in Table 3. Note that the shape factor, K_s

in the second constraint, can be found in the nomenclature of the EJMA standard [2]. It is worth to point out that the stress due to displacement load, S_{10} , is only used in the constraint for the allowable number of cycles, i.e. fatigue constraint. The fatigue curve expression listed in Table 3 is taken from the ASME code [7]. This curve is more conservative than the one provided by EJMA (see Fig. 4.20 in [2]). The ASME fatigue curve is used in our analysis for the purpose of demonstrating the complete procedure.

Table 1. Stresses in rectangular bellows following EJMA standard [2]

Stress component	EJMA Symbol	Equation	Note	Load type
Longitudinal membrane stress	S_7	$\frac{PLq}{2A_c}$	L is length of the other side where S_7 is calculated (*).	Pressure
Longitudinal bending stress	S_{8a}	$\frac{PNqL^2w}{24I}$	L is length of the same side where S_8 is calculated (* and **).	Pressure
Meridional bending stress (sidewall)	S_9	$\frac{P}{2} \left(\frac{w}{t}\right)^2 \left(1 - \frac{1.3r_m}{w}\right)$	-	Pressure
Meridional bending stress (tangent)	S_{11}	$\frac{0.938PL_t^2}{t^2}$	L_t is length of tangent, Fig. 1.	Pressure
Meridional bending stress	S_{10}	$\frac{5E_b te}{3w^2(1 + 3r_m/w)}$	E_b at room T .	Displacement

(*) $L = L_l + w$ or $L_s + 1 + w$

(**) Stress at the ideally stiff corner of a fully clamped beam under pressure load

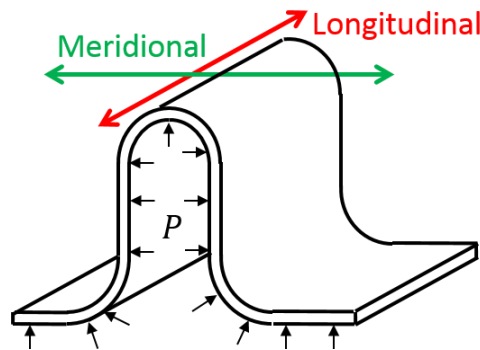


Figure 2: Naming convention of stresses in rectangular bellows relative to the convolution

It is now convenient to define the mean radius and the height (Fig. 1) as:

$$\begin{aligned} r_m &= K_{rm} t \\ w &= K_w r_m. \end{aligned} \quad (1)$$

According to ASME [7], $K_{rm} \geq 3$. The constraint for K_w , given also in Table 3, is purely geometrical.

3 INPUTS AND RESULTS

The analytical procedure described in Section 2 has been implemented into an in-house tool to find the bellows parameters that fulfil the design constraints and minimize the bellows

length and mass. This section describes the input loads and material properties of the bellows and presents the preliminary results of the bellows' dimensioning.

Table 2. Displacements in universal rectangular bellows following EJMA standard [2]

Description	EJMA Symbol	Equation	Note
Axial displacement	e_z	$\frac{U_z}{2N}$	Extension: U_z positive Compression: U_z negative
Equivalent axial movement due to lateral displacement	$e_{t,r}$	$\frac{K_u L U_{t,r}}{2N(L_u - L_b \pm U_z/2)}$	L is length of side parallel to the calculated displacement (*).
Total equivalent axial movement due to extension	ee	$e_z + e_r + e_t$	-
Total equivalent axial movement due to compression	ec	$-e_z + e_r + e_t$	-
Total equivalent axial movement	e	Maximum of ee and ec	-
Maximum equivalent axial extension per convolution	$eemax$	$6r_m - q$	-
Maximum equivalent axial compression per convolution	$ecmax$	$q - 2r_m - nt$	$n=1$ is the number of plies

(*) $L = L_l + w$ or $L_s 1 + w$

Table 3. Bellows design constraints following EJMA [2] and ASME [7] codes

Constraint	Note	Type
$S_7 \leq S_{ab}$	For both, long and short, sides (*).	Limit stress criteria
$S_7 + S_{8a} \leq 1.33K_s S_{ab}$		
$S_9 \leq 1.5S_{ab}$		
$S_{11} \leq 1.5S_{ab}$		
$\left(\frac{2.5}{14.2 \frac{(S_9 + S_{10})}{E_b} - 0.02} \right)^2 \geq N_{cyc}$	E_b at the design temperature	Fatigue
$ee \leq eemax$	-	Geometrical
$ec \leq ecmax$		
$t > 0$		
$K_w \geq 2$		
$K_{rm} \geq 3$		
$N \geq 1$		
$L_c \geq 0$		

(*) $S_{ab} = (2/3) S_{y,min}$

3.1 Bellows dimensions

The bellows shall be placed in the space between the neutron shield of the VV upper port and the cryostat, Fig. 3-left. Based on the 2015 DEMO CAD model (Fig. 3-left), the maximum

length L_u (Fig. 1) of the bellows expansion joint is 4.7 m. The dimensions of the VV upper port cross section, which should be kept available for instrumentation, are given in Fig. 3-right.

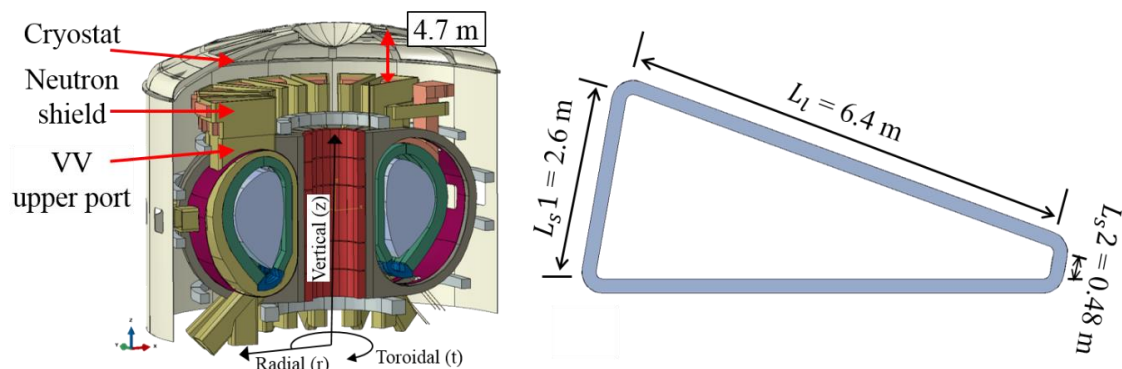


Figure 3: The 2015 global DEMO CAD model, coordinate system of displacements and maximum bellows' length, L_u (left). VV upper port cross section (right).

3.2 Load cases

Table 4 lists the design loads to be analyzed for the DEMO upper port bellows as defined in the task specifications of the project [5]. These include the maximum pressure difference (P) between the internal and external sides of the VV port and the relative displacements between the VV port and the cryostat. The relative displacements are defined in the cylindrical coordinate system of the tokamak defined in Fig. 3-left and include the vertical (U_z), radial (U_r) and toroidal (U_t) displacements. Note that the listed displacements are only approximate, but derived from the DEMO load cases currently assumed [8]. The working temperature (T) of the DEMO VV [9] and the required cycles (N_{cyc}) according to ITER [3] are also given in Table 4.

Table 4. Provisional load cases for the DEMO upper port bellows [5]

Load case*	Load category	Port level	U_z (mm)	U_r (mm)	U_t (mm)	P (MPa)	T (°C)	N_{cyc}
Normal operation	II	Upper	73	35	0	0.15	200	300
Normal operation + VDEIII	III	Upper	73±15	35±34	±36	0.15	200	10

*Effect of gravity is considered in all load cases.

3.3 Materials

Two typical materials for the construction of bellows expansion joints are considered, i.e. stainless steel (SS) 304L and Inconel 625. Table 5 lists their material properties relevant for the design of bellows at room and design temperatures. Note the higher yield stress of Inconel 625.

Table 5. Properties for the bellows materials [10]

Property	Symbol	Temperature (°C)	SS 304L	Inconel 625
Yield stress (MPa)	$S_{y,min}$	20	180	414
		200	118	377
Young Modulus (GPa)	E_b	20	200	207
		200	185	197

3.4 Results of the analytical procedure

The rectangular bellows with dimensions $L_l = 6.4$ m and $L_{s1} = 2.6$ m (Fig. 3-right) and without tangent material ($L_t = 0$ in Fig. 1) are assumed. The total length of the bellows, L_u in Fig. 1, is an input to the procedure. The results in this section are then presented as the regions, within in the three dimensional space designated by K_{rm} , K_w and N , where the design constraints are fulfilled for a given thickness t . Additionally, the colors in individual plots represent either the mass or the connector's length, L_c , for a selected set of parameters. The bellows mass can be readily calculated assuming the typical density for steels of $8,000$ Kg/m³.

The results shown in Figs. 4-6 are obtained, respectively, for $t=3, 5$ and 10 mm, assuming an input $L_u=4.7$ m, the Normal Operation (NO) loads in Table 5 and Inconel 625 material. For $t=3$ mm in Fig. 4, the region of available parameters is rather small in terms of available K_{rm} and K_w . However, the number of convolutions N varies from approximately 2 up to 60. The mass increases with N up to 25 tonnes. On the other hand, L_c decreases for increasing N , i.e. higher the number of convolutions, shorter the connector. For $t=5$ mm in Fig. 5 the region of available K_{rm} and K_w parameters increases substantially. For low K_{rm} , a wide range of K_w and N may be chosen with bellows masses ranging from 5 to 25 tonnes and L_c from very short to more than 3 m. For increasing K_{rm} , the possible K_w and N available values get reduced. For $t=10$ mm in Fig. 6, the region shrinks but reaches higher values of K_{rm} . Bellows of such thicknesses, however, are clearly heavier and not necessarily optimal from a material and fabrication costs point of view. The results for the same input length of 4.7 m but under NO+VDEIII load conditions (Table 4) are practically identical to those in Figs. 4-6 and are not shown.

Figure 7 shows the results for the same case as in Fig. 6 but assuming SS 304L material. It is clearly shown that the region of available parameters gets reduced due to the lower yield stress of the material. With SS 304L, no available parameters is found for t lower than 10 mm. Figure 8 shows the results assuming now the bellows total length of $L_u=2$ m, NO loads, $t=5$ mm and Inconel material. The effects of shorter bellows can be seen through comparison with Fig. 5. Clearly, the available region of parameters is smaller. Moreover, for the assumed $L_u=2$ m, the more challenging NO+VDEIII input load have now an effect on the region parameters. This is shown in Fig. 9, where it can be seen that the available parameters are grouped in disconnected regions. The developed analytical tool enables to identify a valid range of parameters and, at the same time, to optimize the bellows mass and length. This would be a rather challenging task if based on finite element simulations only.

4 CONCLUSIONS

A preliminary dimensioning of the DEMO upper port duct bellows has been performed with the available analytical procedures for rectangular bellows design. The development of an optimization tool for bellows parameters has also been initiated. The results of the analyses show that, with the current design assumptions, the available sets of bellows parameters are very dependent on the inputs. It has also been found that the high mass of some of the available bellows may represent an important design constraint.

ACKNOWLEDGMENTS

This work has been carried out within the framework of the EUROfusion Consortium and has received funding from the Euratom research and training programme 2014–2018 under grant agreement No. 633053. The views and opinions expressed herein do not necessarily reflect those of the European Commission.

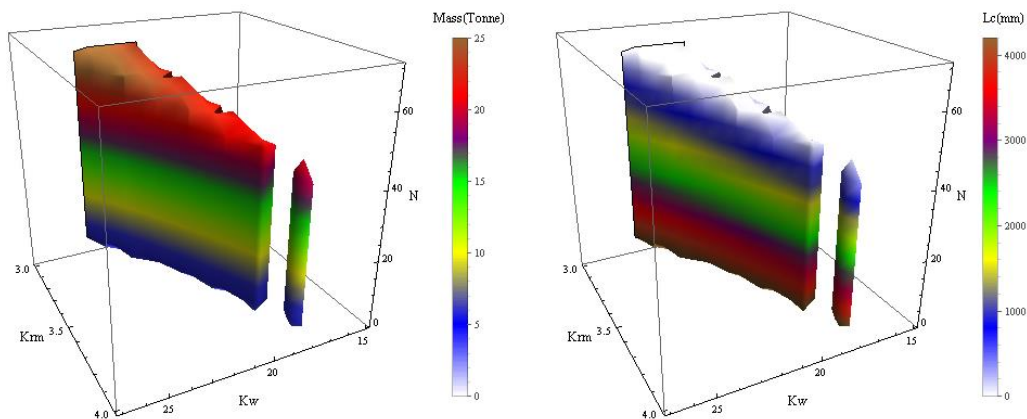


Figure 4: Parameters space for NO, $t=3$ mm, $L_u=4.7$ m and Inconel

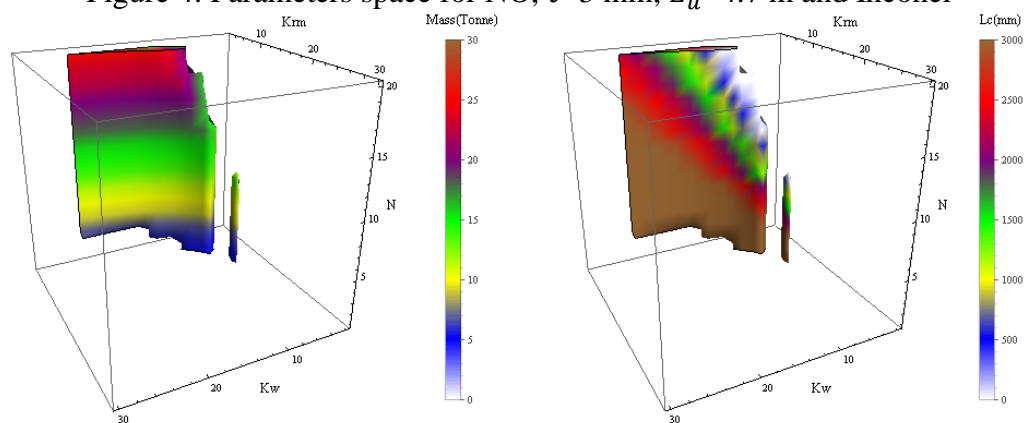


Figure 5: Parameters space for NO, $t=5$ mm, $L_u=4.7$ m and Inconel

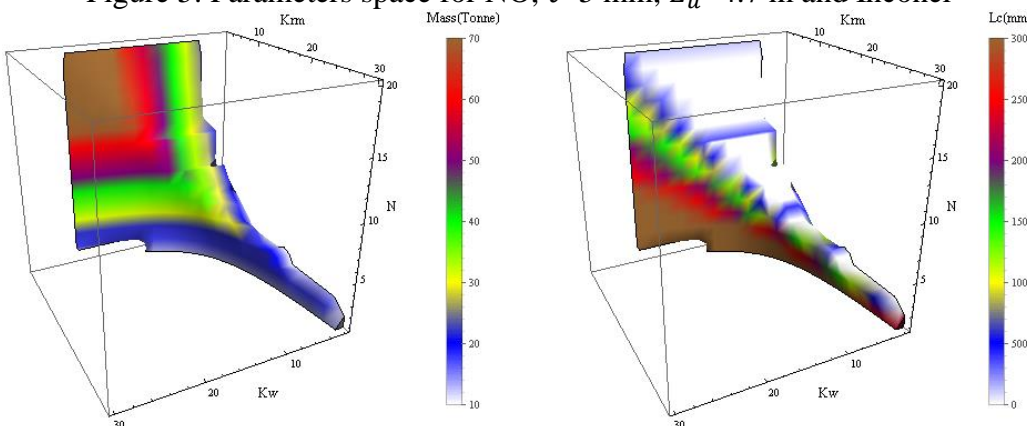


Figure 6: Parameters space for NO, $t=10$ mm, $L_u=4.7$ m and Inconel

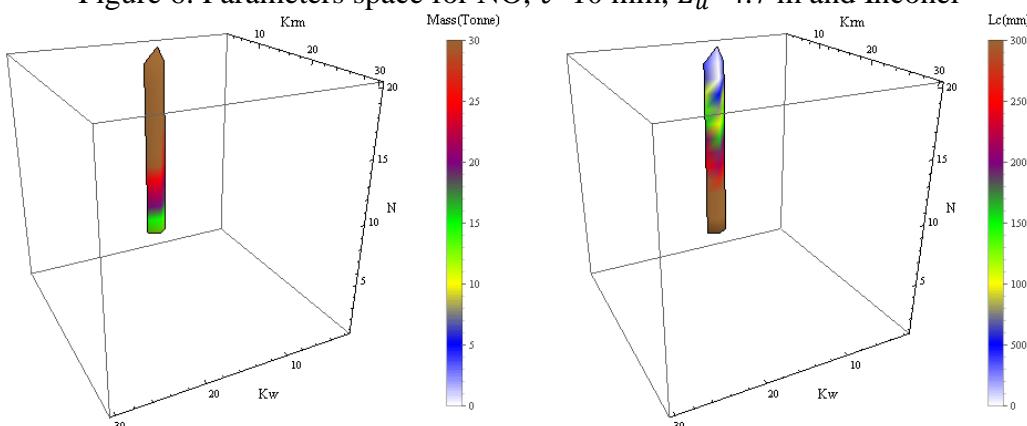


Figure 7: Parameters space for NO, $t=10$ mm, $L_u=4.7$ m and SS 304L

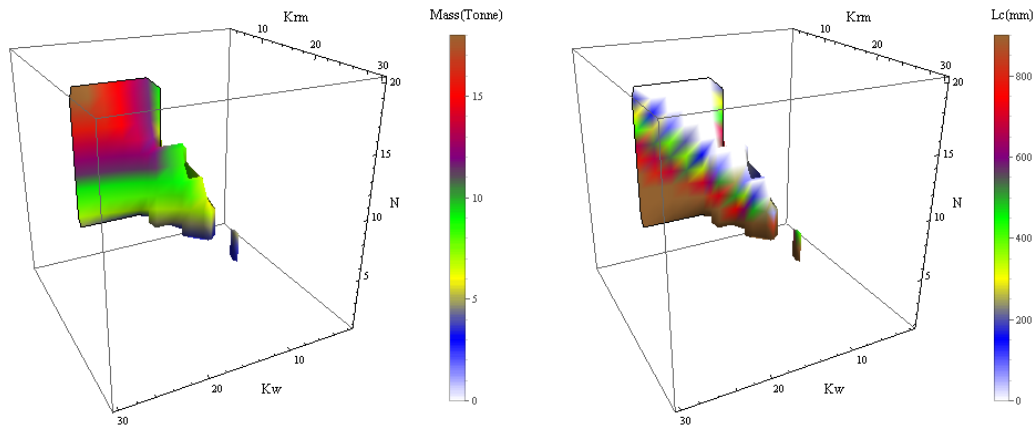


Figure 8: Parameters space for NO, $t=5$ mm, $L_u=2.0$ m and Inconel

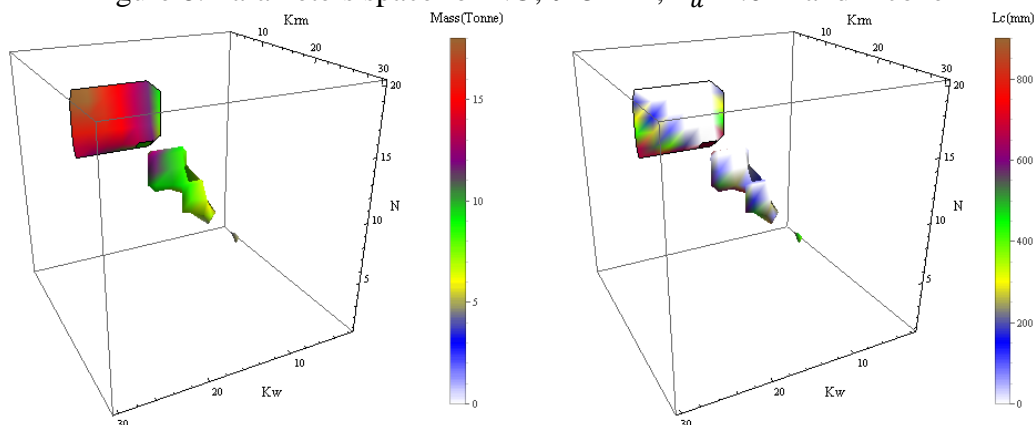


Figure 9: Parameters space for NO+VDEIII, $t=5$ mm, $L_u=2.0$ m and Inconel

REFERENCES

- [1] ASME, "American Society of Mechanical Engineers, Section VIII - Division I, rules for construction of pressure vessels", Section VIII - Division I, rules for construction of pressure vessels, NY, USA, 2007.
- [2] EJMA, "Standards of the expansion joint manufacturers association, inc.", New York, USA, 2008.
- [3] H. Xie, "Kompaflex final report of rectangular bellows for ITER cryostat system", PNTALJ, ITER, 2014.
- [4] J. Reich, et al., "Experimental verification of the axial and lateral stiffness of large W7-X rectangular bellows", Fusion Engineering and Design, 82, 2007, pp. 1924-1928.
- [5] R. Brown, "Further development of DEMO TS concepts and initial definition of cryostat bellows", EFDA_D_2MQDA4, EUROfusion, 2016.
- [6] O. Costa Garrido, B. Končar, "Initial Definition and Analysis of the DEMO Cryostat Bellows", EFDA_D_2MQXKB, JSI, 2017.
- [7] ASME, "Companion guide to the ASME Boiler & Pressure Vessel code, Volume 2, Chapter 21: Section VIII - Division I, rules for construction of pressure vessels", NY, USA, 2002.
- [8] C. Bachmann, et al., "Initial definition of structural load conditions in DEMO", Fusion Engineering and Design, <http://dx.doi.org/10.1016/j.fusengdes.2017.02.061>, 2017.
- [9] B. Končar, et al., "Thermal analysis of DEMO tokamak 2015", EFDA_D_2LAL73, JSI, 2016.
- [10] V. Barabash, "Appendix A, Materials design limit data", 222RLN, ITER, 2013.